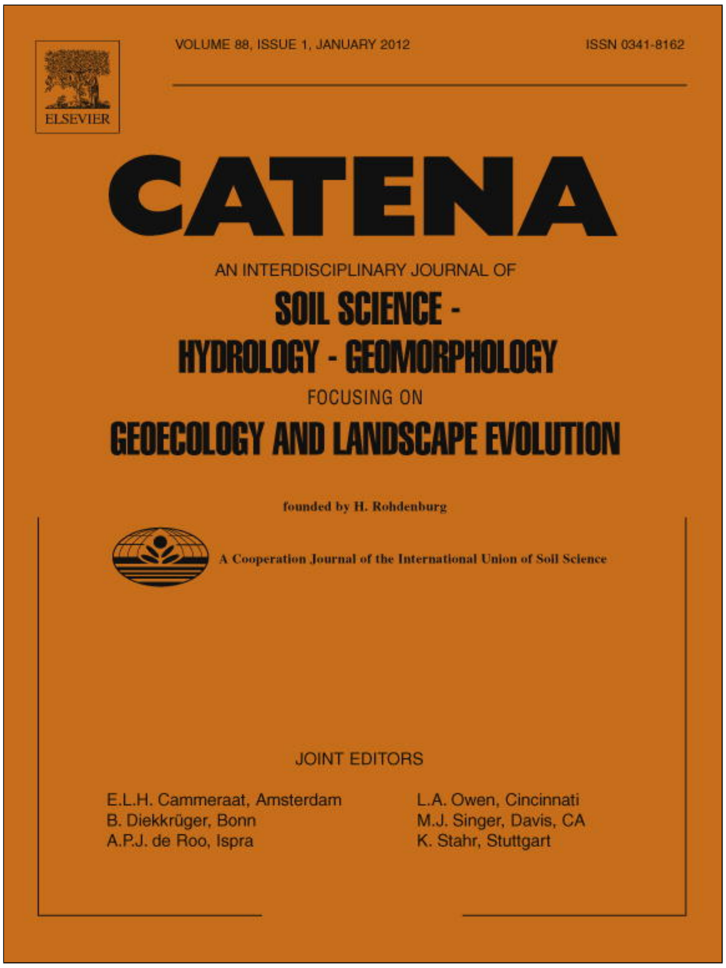

(This is a sample cover image for this issue. The actual cover is not yet available at this time.)

Catena 92 (2012) 196–207

Contents lists available at SciVerse ScienceDirect

Catena

journal homepage: www.elsevier.com/locate/catena

Minero-petrographical features of weathering profiles in Calabria, southern Italy

L. Borrelli [a], F. Perri [b,*], S. Critelli [b], G. Gullà [a]

[a] CNR-IRPI_U.O.S. di Cosenza, Via Cavour n. 4/6, 87030 Rende (CS), Italy
[b] Università degli Studi della Calabria, Dip. Scienze della Terra, 87030 Rende (CS), Italy

ARTICLE INFO

Article history:
Received 15 January 2011
Received in revised form 9 January 2012
Accepted 11 January 2012
Available online xxxx

Keywords:
Weathering
Clay minerals
Petrography
Soil micromorphology
Gneiss

ABSTRACT

The paper reports interdisciplinary research of weathering profile stages on gneiss with regard to tectonic and landscape evolutions of the western Sila Grande Massif (Southern Italy). The outcropping rocks consist of medium- to coarse-grained biotite–garnet and sillimanite gneiss (BGS-G), and medium- to coarse-grained biotite–muscovite migmatitic gneiss (M-G). The BGS-G rocks are fractured and weathered with either massive or foliated texture, whereas the M-G rocks are intensely weathered and fractured with a massive texture and frequent pegmatite veins. Petrographical and mineralogical variations show that both gneissic rocks (BGS-G and M-G samples) underwent weathering processes characterized by a progressive chemical attack on the labile minerals with generation of neoformed minerals and substitution of the original rock fabric. The weathering processes produced phyllosilicates and Fe-oxides; neoformed clay minerals and ferruginous products replaced feldspars and biotite during the most advanced weathering stage. Microfractures and morphological variations occur on the original rock and, thereby, affect the surrounding landscape processes. The weathering profile mineralogy and rock textures viewed in the context of landscape evolution provide useful insights into the widespread slope movement phenomena in the Sila Grande Massif gneiss.

1. Introduction

Certain Italian regions (e.g., Alps, Calabria and Sardinia) are occupied with crystalline rocks which have undergone intense weathering processes. Due to the combination of several predisposing morpho-lithological, tectonic and climatic factors, intense weathering and related slope instability are very common. Generally, weathering produces mineralogical and petrographical transformations and, thus, a considerable decay of the physical–mechanical properties of the original rock, predisposing the slope instability processes (e.g., Borrelli, 2008; Borrelli et al., 2007; Brand and Phillipson, 1985; Calcaterra et al., 1996, 2004; Cascini and Gullà, 1993; Cascini et al., 1992, 1994; Critelli et al., 1991; Deere and Patton, 1971; Gullà et al., 2004; Hencher et al., 1984; Lacerda and Santos, 2000; Nishida and Aoyama, 1985). The weathering phenomena are, furthermore, closely related to geological engineering projects and anthropic interventions (e.g., Gullà et al., 2008).

The main mountainous massifs of the Calabria region (southern Italy) are characterized by outcropping of crystalline rocks. In particular, intense weathering processes have developed in the crystalline rocks characterized by granitic and gneissic compositions (Guzzetta, 1974). Weathering and erosion vary markedly across the Sila Massif (northern Calabria) according to the topographic setting. The central portion of the massif is dominated by a broad upland plateau where weathering exceeds the rate at which slope processes can remove detritus (Le Pera et al., 2001). A thick soil cover is present here in flat depressions, gentle slopes and flat hilltops (Le Pera and Sorriso-Valvo, 2000b). The highland plateau abruptly passes into valley slopes with sharp slope gradient. The steeper slopes are subject to frequent landslides (Borrelli, 2008; Cascini et al., 1992), and mechanical erosion is more pronounced than chemical weathering (Le Pera and Sorriso-Valvo, 2000a). In these positions, the dynamics of weathering is strongly controlled by relief characteristics (e.g., Teeuw et al., 1994; Thomas, 1994).

This paper presents results of a multidisciplinary study (e.g., Borrelli, 2008; Borrelli et al., 2007) on the weathering profile evolution, carried out in the area of ca. 70 km^2, situated in the central sector of the Mucone River basin, on the north-western slopes of the Sila Massif (northern Calabria) (Fig. 1). This work aims to examine the physical, mechanical and mineralogical–petrographical properties of both parent/fresh rocks and weathered rocks of the gneissic slopes of the Sila Massif. The application of soil micromorphology (Stoops, 2003) to weathering phenomena proved to be useful. The studied area is chiefly formed by weathered gneiss characterized by significant instability phenomena, although sometimes recognizable with difficulty. Weathering of rocks involves several processes such as dissolution of primary phases, deposition of authigenic minerals, ionic exchange and sorption. These processes are dependent on the chemistry and mineralogy of the rocks, chemical features of the interacting

* Corresponding author.
E-mail addresses: francesco.perri@unibas.it, perri@unibas.it (F. Perri).

0341-8162/$ – see front matter
doi:10.1016/j.catena.2012.01.003

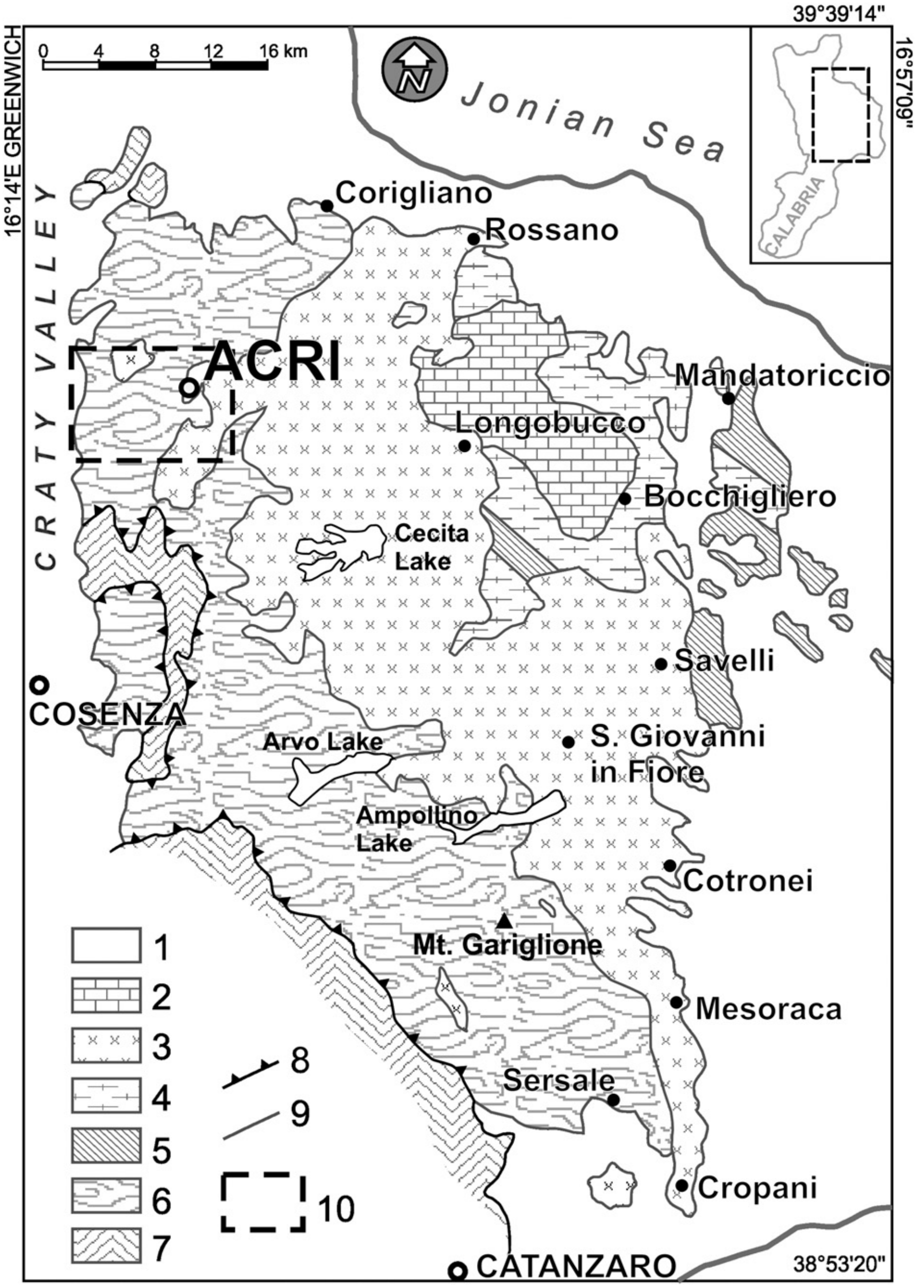

Fig. 1. Geologic sketch of the Sila Massif (modified from Messina et al., 1991) with location of the study area. Legend: 1) predominantly clastic deposits (Recent to Tortonian). 2 to 6 = Sila Unit: 2) Mesozoic to Tertiary sedimentary cover; 3) plutonic rocks (Sila Batholith; Carboniferous–Permian); 4) low-grade metamorphic rocks (Bocchiglero Complex; Late Cambrian to Early Carboniferous); 5) low- to medium-grade metamorphic rocks (Mandatoriccio Complex; Late Cambrian to Early Carboniferous); 6) medium- to high-grade metamorphic rocks (Monte Gariglione–Polia-Copanello Complex; pre-Triassic); 7) Lower Alpine thrust nappes of the Sila Massif including Castagna, Bagni and Ophhiolitic Units (phyllite + schist and ophiolitic rocks); 8) thrust fault; 9) stratigraphic contact; 10) studied area.

waters and on physical and biological factors such as topography, climate, and biological activity.

The approach used and the results proposed in this paper provides a valuable support for the study of mass movement phenomena related to different geological contexts mainly characterized by weathered crystalline rocks, and for the mechanical characterization of weathering profiles.

2. Geological and geomorphological features

The studied area is located on the western side of the Sila Massif (Fig. 1). This area represents a section of the Hercynian orogenic belt of western Europe, were allochthonous crystalline basement rocks are exposed to form the highest tectonic units (Calabrian Arc) of the southern Italy fold–thrust belt (Amodio-Morelli et al., 1976). The Sila Massif consists of Paleozoic intrusive and metamorphic rocks, locally unmetamorphosed, with a Mesozoic sedimentary cover. The Paleozoic rocks consist of gneiss, amphibolite, schist and phyllite, affected by various Alpine metamorphic events and intruded by the Late Hercynian Sila Batholith (Messina et al., 1991, 1994). Gneissic rocks consist of biotite–sillimanite–garnet-rich layers with both massive and migmatitic structures. Contacts among gneissic rocks and Sila Batholith are marked by a network of pegmatite dikes and by an irregular thermal aureole with amphibolite facies (Caggianelli et al., 1994). The Sila Batholith consists of multiple intersecting intrusions, heterogeneous in texture and fabric, with a composition ranging from granodiorite to gabbro and leucomonzogranite (Messina et al., 1991). Fission track analyses of apatite and zircon from the basement rocks of the Sila Massif indicate a major period of exhumation ranging from ca. 35 Myr to ca. 15 Myr (Thomson, 1994).

The sampling area is located in the central sector of the Mucone River basin, on the north-western slope of the Sila Massif (northern Calabria) (Fig. 2). It extends about 70 Km^2 and ranges in elevation from 200 to 950 m asl. The climate is upland Mediterranean-type (Cbs, sensu Köppen, 1936), with hot, dry summers and precipitations concentrated in mild winters. The drainage network is mainly controlled by the discontinuities produced by Quaternary tectonics. The drainage system is dense and often cuts the bedrock (e.g., Cascini et al., 1992). The investigated area shows the evidence of glacial events, probably belonging to the last glacial age (Late Würm), between 21,000 and 18,000 B.P. (Palmentola et al., 1990), which contributed to shape its main morphologies. Three main morphological sectors may be distinguished: the highplains, the main slope, and the valley. Highplains are the highest and most ancient tabular surfaces, where weathering processes are essentially of the chemical type. They are morphodynamically inactive, with the exception of slow in situ rock alteration. The main slopes show high gradient values (about 35°–40°). This is the sector where erosion and mass movement are particularly widespread. Slope movement typologies are commonly rock-slide, soil-slips and debris-flows, with subordinate other types of landslides (Borrelli, 2008; Terranova et al., 2007). The valley is mostly characterized by sedimentation, but local erosion can also be observed.

The studied rocks are characterized by Paleozoic gneiss of the Monte Gariglione–Polia-Copanello Complex and consist of medium- to coarse-grained biotite–garnet and sillimanite gneiss (BGS-G), outcropping along the Mucone River, and medium- to coarse-grained biotite–muscovite migmatitic gneiss (M-G), outcropping close to the contact with the plutonic rocks (Sila Batholith). The BGS-G samples are fractured and weathered showing either massive or foliated texture; the M-G samples are intensely weathered and fractured showing a massive texture with frequent pegmatite veins. The metamorphic rocks are often covered with colluvial deposits of variable thickness.

The severe fracturing, mainly related to neotectonic activity of the massif uplift, favors chemical alteration and physical degradation which both play an important role in the evolution of landslide phenomena (e.g. Cascini et al., 1992). The resulting weathering profiles, typical of a wide area in the Sila Massif, are from ca. 20 m to ca. 60 m thick. The weathering profiles are quite complex and irregular showing frequent lateral and vertical variations (e.g., Borrelli et al., 2007; Calcaterra et al., 1998; Cascini et al., 1992; Deere and Patton, 1971).

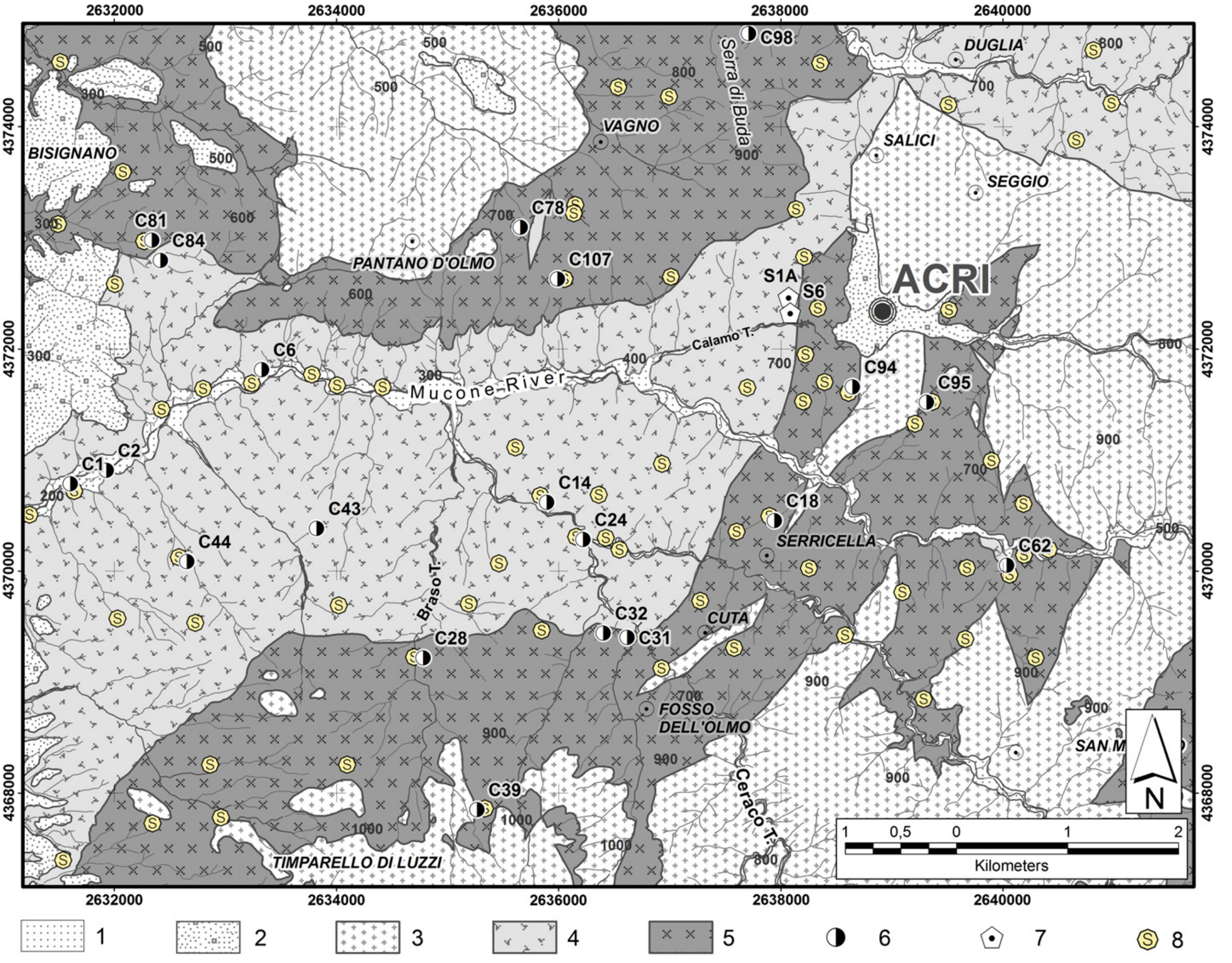

Fig. 2. Simplified geological map of the Acri studied area. Legend: 1) alluvial deposits; 2) matrix-supported conglomerates (Lower–Middle Pleistocene); 3) granitoids rocks (Paleozoic); 4) biotite–garnet–sillimanite gneiss (Paleozoic); 5) biotite–muscovite migmatitic gneiss (Paleozoic); 6) sampling from cut slope weathering profiles; 7) sampling from 150-meter-long boreholes; 8) studied weathering profiles.

3. Weathering grade surveys

A preliminary study of the cut slopes has been carried out following the methodology proposed by Gullà and Matano (1994, 1997). Based on this methodology, six classes of weathering have been recognized: class VI (residual and colluvial soils), class V (completely weathered rock), class IV (highly weathered rock), class III (moderately weathered rock), class II (slightly weathered rock) and class I (fresh rock). Class VI groups both the loose rocks formed by the weathering processes in situ (residual deposits) and the soils made up of weathered material transported by slope processes (colluvium) which were found in abundance during the study (e.g., Cascini et al., 1994).

The weathering profiles have been reconstructed based on the main cut slopes observed (Fig. 3). The cut slopes have been examined to get information about the thickness and features of weathering profiles. The cut slope study shows that the BGS-G samples are characterized by complex weathering profile, where moderately weathered rocks (class III) and highly weathered rocks (class IV) prevails. The cut slopes of the M-G area are complex and characterized by intense weathering processes where class V weathered rocks prevail.

The general weathering conditions are associated with intense fracturing determined by joints, thrust faults and some normal fault planes (Fig. 3). Moreover, it is possible to observe fault gauge along some fault planes (Fig. 3).

In order to obtain indications on the vertical variations of the studied weathering horizons, the surveys on the cut slopes were integrated with a stratigraphic analysis of 8 continuous boreholes, which were grilled up to 150 m (Fig. 4) in the studied area (Fig. 2).

The analysis of the borehole logs, obtained by the geotechnical sounding (Sorriso-Valvo et al., 2005), shows that the weathered rock thickness is at least 60 m (Fig. 4). The analysis of these data permits to define the weathering profile features of the studied area (Fig. 5). The weathering profiles show clear transitions among class VI and class II, class VI and class IV, and class IV and class II (Fig. 5). Thin and discontinuous horizons of completely weathered rocks

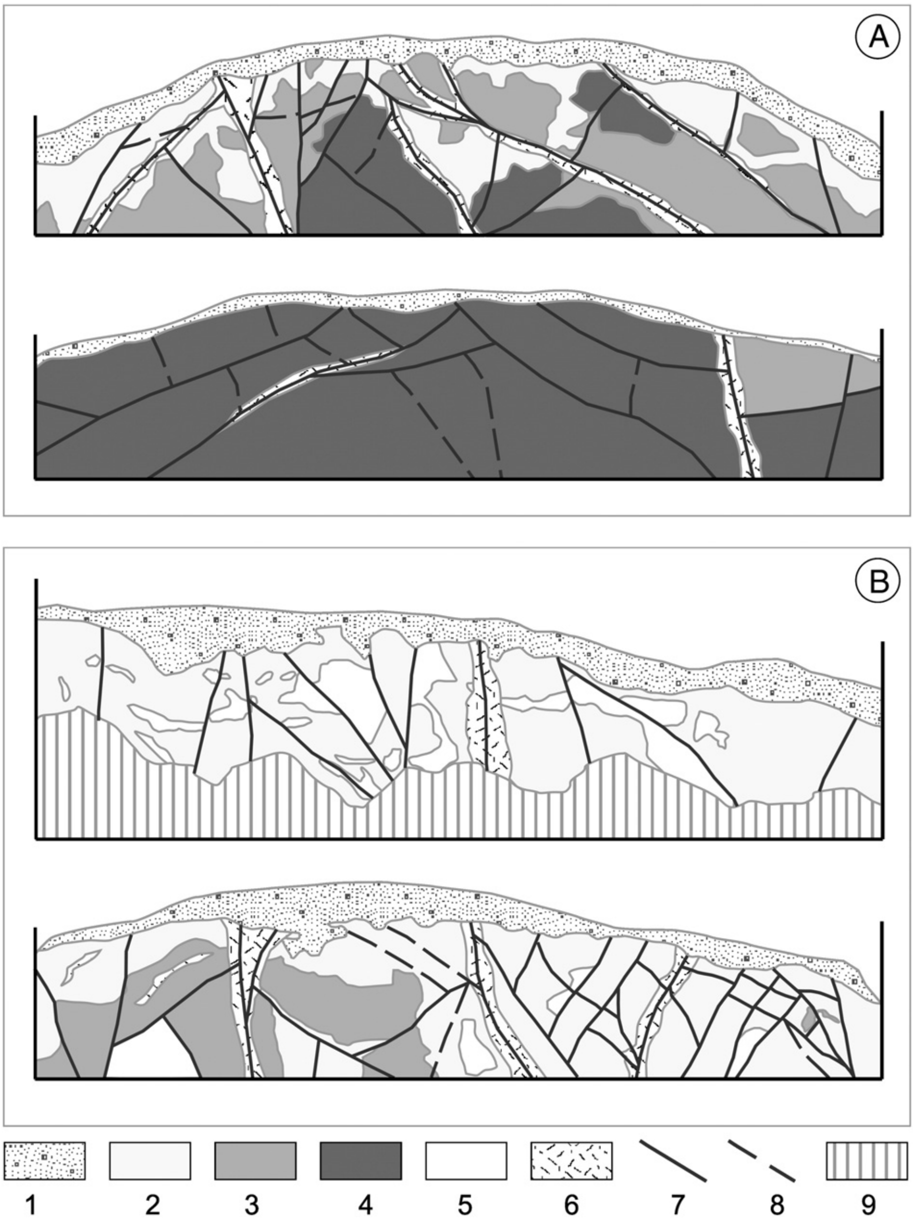

Fig. 3. Weathering profiles of representative cut slopes of the studied area: A) weathering profiles of the BGS-G rocks; B) weathering profiles of the M-G rocks. Legend: 1) residual and colluvial soils (class VI); 2) completely weathered gneiss (class V); 3) highly weathered gneiss (class IV); 4) moderately weathered gneiss (class III); 5) pegmatite; 6) fault gouge; 7) fault; 8) fracture; 9) vegetation cover.

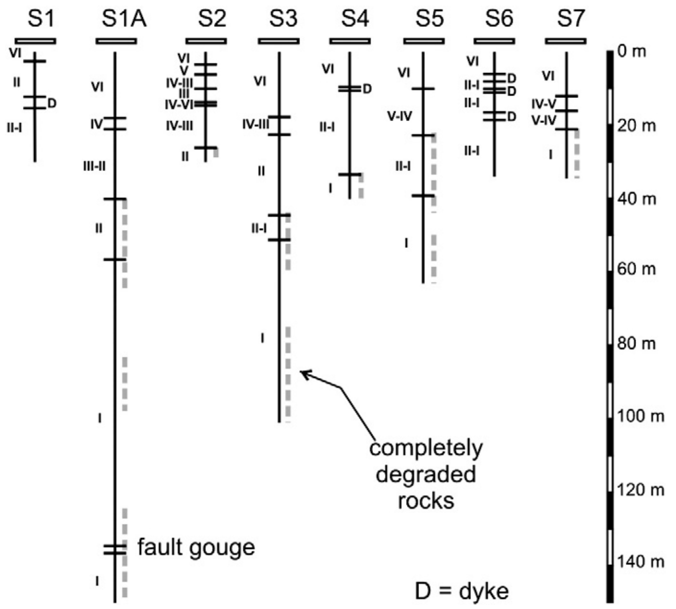

Fig. 4. Weathering grade in the borehole logs. Legend: class VI (colluvial cover); class V (completely weathered rock); class IV (highly weathered rock); class III (moderately weathered rock); class II (slightly weathered rock); class I (fresh rock).

(class V), highly weathered rocks (class IV) and moderately weathered rocks (class III) occur in the studied profiles (Fig. 5).

The weathering profile of the studied area shows horizons characterized by completely degraded rocks, sometimes argillified, associated with thrust planes (Fig. 5). Furthermore, the studied profiles are characterized by cataclastic zones in correspondence of normal faults; in these zones the rocks range from very fractured to heavily fractured with completely weathered portions (Fig. 5).

4. Sampling and methods

Samples were collected from both 150-meter-long boreholes (4 samples at various borehole depths; Table 1) and along weathering profiles during the field survey (20 samples; Table 1), around the Acri village, on the western slope of the Sila Massif (northern Calabria), which provides a continuous record from fresh metamorphic rocks to weathered soil profiles (Fig. 2).

Samples were thin sectioned for petrographic analysis. The progress of weathering has been characterized through calculation of the decomposition index (X_d; Lumb, 1962), indicating the extent to which the rock microfabric and composition are affected by weathering, leading to soil formation. This index, according to Lumb (1962), has been defined as $X_d = N_q - N_{q0}/1 - N_{q0}$, where N_q is the weight ratio of quartz and feldspar in the soil sample, N_{q0} is the weight ratio of quartz and feldspar in the original rock. N_q has been determined by separating the grains by hand picking under an optical microscope using the soil fraction retained on a 500-μm aperture sieve. N_q was obtained by artificial crushing of the original bedrock. This artificially crushed rock was successively dry sieved to obtain the same sand fraction (500 μm) as the associated soil samples.

A selection of the original uncrushed bedrock samples was also used for calculating the micropetrographic index (I_p; Irfan and Dearman, 1978), to assess different stages of weathering (e.g., Irfan and Dearman, 1978; Tsidzi, 1986). This index is defined as $I_p =$% sound constituents/% unsound constituents, where sound constituents are primary and accessory unaltered minerals, and unsound constituents are secondary minerals such as clay minerals, chlorite, sericite, iron-oxides, together with microcracks and voids.

The studied samples have been also investigated by scanning electron microscope (SEM) on the fractured surfaces; analyses were performed on a FEI Quanta 200 Scanning Electron Microscope equipped with EDAX Genesis 4000, at the Università della Calabria (Italy).

Furthermore, mineral composition was determined for both fresh and completely weathered rock samples, using X-ray powder diffraction (XRD; Bruker D8 Advance diffractometer, with CuKα radiation in the range of 5°–60° 2θ, with steps of 0.02° 2θ and step-times of 1 s/step) at the Università della Calabria (Italy). X-ray diffraction analyses were carried out according to Moore and Reynolds (1997). The occurrence of phyllosilicates in the bulk rock was split on the diffraction profile of the random powder, according to the following peak area: 10–15 Å (interstratified clay minerals), 10 Å (illite + micas), and 7 Å (kaolinite + chlorite) minerals (e.g., Cavalcante et al., 2007; Perri, 2008).

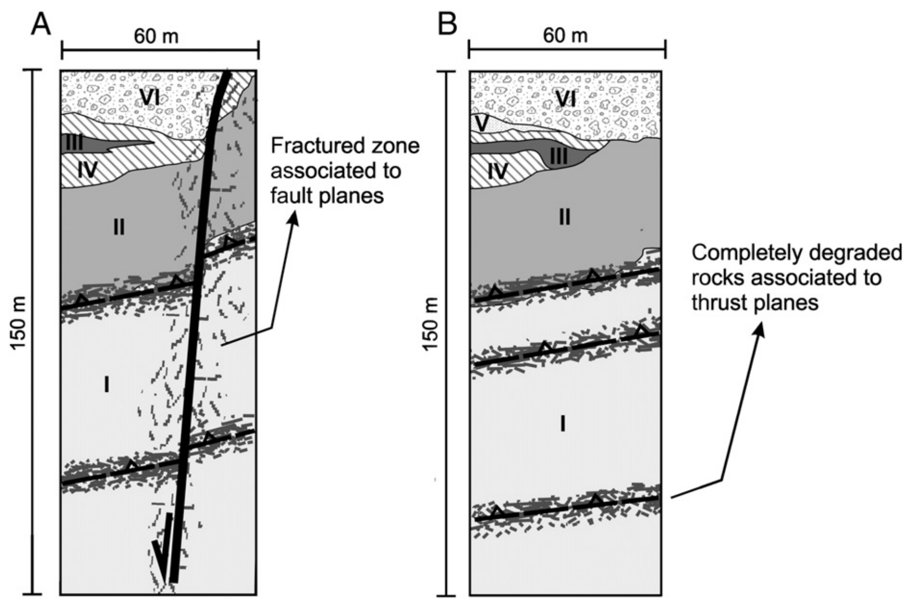

Fig. 5. Schematic distribution of the typical weathering profiles of the study area.

Table 1
Characterization of studied gneiss in terms of composition, decomposition index (X_d; Lumb, 1962), microfabric, micropetrographic index (I_p; Irfan and Dearman, 1978) and weathering stages.

Sample no.	Type of gneiss	Decomposition index (*Xd*)	Microfabric	Micropetrographic index (*Ip*)	Weathering stage
C1	Bt + grt + sill gneiss (BGS-G)	–	Granular-framework	4.87	III
C2	Bt + grt + sill gneiss (BGS-G)	0.38	Granular-framework	2.99	IV
C6	Bt + grt + sill gneiss (BGS-G)	–	Granular-framework	13.06	I
C14	Bt + grt + sill gneiss (BGS-G)	-	Granular-framework	7.67	II
C24	Bt + grt + sill gneiss (BGS-G)	–	Granular-framework	4.85	III
C43	Bt + grt + sill gneiss (BGS-G)	0.5	Clay-matrix	1.9	IV–V
C44	Bt + grt + sill gneiss (BGS-G)	0.56	Clay-matrix	0.88	V
C84	Bt + grt + sill gneiss (BGS-G)	0.26	Granular-framework	2.8	IV
SIA-1 (20 m borehole depth)	Bt + grt + sill gneiss (BGS-G)	0.16	Granular-framework	4.21	III
SIA-2 (22 m borehole depth)	Bt + grt + sill gneiss (BGS-G)	0.39	Granular-framework	3.32	IV
SIA-3 (48 m borehole depth)	Bt + grt + sill gneiss (BGS-G)	0.18	Granular-framework	2.91	IV
SIA-4 (147 m borehole depth)	Bt + grt + sill gneiss (BGS-G)	–	Granular-framework	14.04	I
C18	Migmatitic gneiss (M-G)	0.92	Clay-matrix	0.25	V
C28	Migmatitic gneiss (M-G)	0.55	Clay-matrix	0.43	V
C31	Migmatitic gneiss (M-G)	1	Clay-matrix	0.65	V
C32	Migmatitic gneiss (M-G)	0.93	Clay-matrix	0.73	V
C39	Migmatitic gneiss (M-G)	0.79	Clay-matrix	0.31	V
C62	Migmatitic gneiss (M-G)	0.21	Granular-framework	2.12	IV
C78	Migmatitic gneiss (M-G)	–	Granular-framework	14.17	I
C81	Migmatitic gneiss (M-G)	–	Granular-framework	6.33	II
C94	Migmatitic gneiss (M-G)	–	Granular-framework	12.26	I
C95	Migmatitic gneiss (M-G)	0.97	Clay-matrix	0.39	V
C98	Migmatitic gneiss (M-G)	0.48	Clay-matrix	1.55	IV–V
C107	Migmatitic gneiss (M-G)	0.85	Clay-matrix	1.8	IV–V

5. Results

5.1. Rock composition

The studied gneiss can be grouped in two main groups: the first one characterized by biotite, garnet and sillimanite gneiss (BGS-G), and the second characterized by biotite–muscovite migmatitic gneiss (M-G) (Table 1).

The BGS-G samples are medium- to coarse-grained with a granolepidoblastic texture, and are composed of plagioclase, quartz, biotite, iron-bearing garnet (almandine), sillimanite and K-feldspar; minor zircon, apatite, epidote and opaques that occur as accessory minerals. Both garnet and biotite show frequently neoformation of ferruginous weathering product as linings within and around crystals.

The M-G samples are medium- to coarse-grained, having a granoblastic texture and consist of quartz, plagioclase, biotite, muscovite and chlorite and, rarely, sillimanite and garnet; minor zircon, apatite, epidote and opaques that occur as accessory minerals.

The weathered horizons along the weathering profiles are mainly characterized by both mineral alteration and textural change.

5.2. Assessment of weathering processes

Grade of physical disintegration and chemical alteration of rocks (weathering susceptibility) is mainly dependent on environmental factors, such as climate, hydrogeology, biology and morphology, as well as on the nature of the parent rock and physico-mechanical and geomechanical properties (e.g., Hill and Rosenbaum, 1998; Price, 1995).

Based on guidelines given in earlier studies, we assessed chemical and minero-petrographical indices of the weathering process (e.g., Baynes and Dearman, 1978a; Caracciolo et al., 2011; Critelli et al., 2008; Fedo et al., 1995; Irfan and Dearman, 1978; Lee and De Freitas, 1989; Le Pera and Sorriso-Valvo, 2000a, 2000b; Le Pera et al., 2001; Lumb, 1962; Mongelli et al., 1998, 2006; Nesbitt and Young, 1982; Perri, 2006; Perri et al., 2005, 2008, 2011; Tsidzi, 1986; Zaghloul et al., 2010 and many others).

The fresh rock is generally characterized by unaltered minerals, without Fe-oxide formation and granular disintegration (Fig. 6A). The weathered samples preserve the texture of the parent rock, even if most of the rocks have a deep-brown iron-staining. The transition from slightly weathered samples (Fig. 6B–C) to highly weathered (Fig. 6D) and completely weathered samples (Fig. 6E–F) is marked by both granular disintegration and chemical alteration. At the same time, significant aperture of microcracks and contacts among minerals, with the tendency to lose their original crystalline habit, were observed. The main mineralogical changes of weathered gneiss concern the argillification (with neoformation of clay minerals) of plagioclase (Fig. 7A), Fe-oxide replacement in biotite (Fig. 7B) and chloritization, mineral dissolution (Fig. 7C), and new formation of platy illite and illite/smectite (Fig. 7D), kaolinite (Fig. 7E) and halloysite (Fig. 7F). Furthermore, an incipient disintegration, indicated by transgranular and intragranular microcracks (Fig. 7B–G), as well as chemical alteration, characterizes feldspar grains as showed by SEM images (Fig. 7H). Halloysite, together with kaolinite, has been previously identified as a possible feldspar derivative occurring on Sila Massif weathered gneiss (Critelli et al., 1991; Le Pera et al., 2001).

Thus, the completely weathered stage is marked by an increase in chlorite, appearance of clayey minerals with feldspars and biotite highly altered and fractured owing to opening of microcracks (e.g., Fig. 7B).

Petrographic analysis based on the X_d values (Lumb, 1962) and the micropetrographic index I_p (Irfan and Dearman, 1978) have been carried out on the studied gneiss samples (Table 1).

The BGS-G samples generally show low X_d values and are characterized by granular-framework microfabric (Baynes and Dearman, 1978b); the X_d value is not detected for the fresh and the slightly weathered samples (classes I and III) (Table 1). The M-G samples show X_d values that range from 0.21 to 1. These samples are generally characterized by clay-matrix microfabric (Baynes and Dearman, 1978b); the samples showing lower or not detected X_d values, have granular-framework microfabric (Table 1). The granular-framework microfabric consists of an interlocking granular aggregate enclosing isolated, decomposed minerals, and is clay-poor, whereas, the clay-matrix microfabric is typical of a rock where decomposition products, mainly clayey phases, dominate and enclose the remnant original minerals.

Based on the micropetrographic index I_p (Irfan and Dearman, 1978), two main stages (classes IV and V; e.g., Fig. 6D–F) weathering

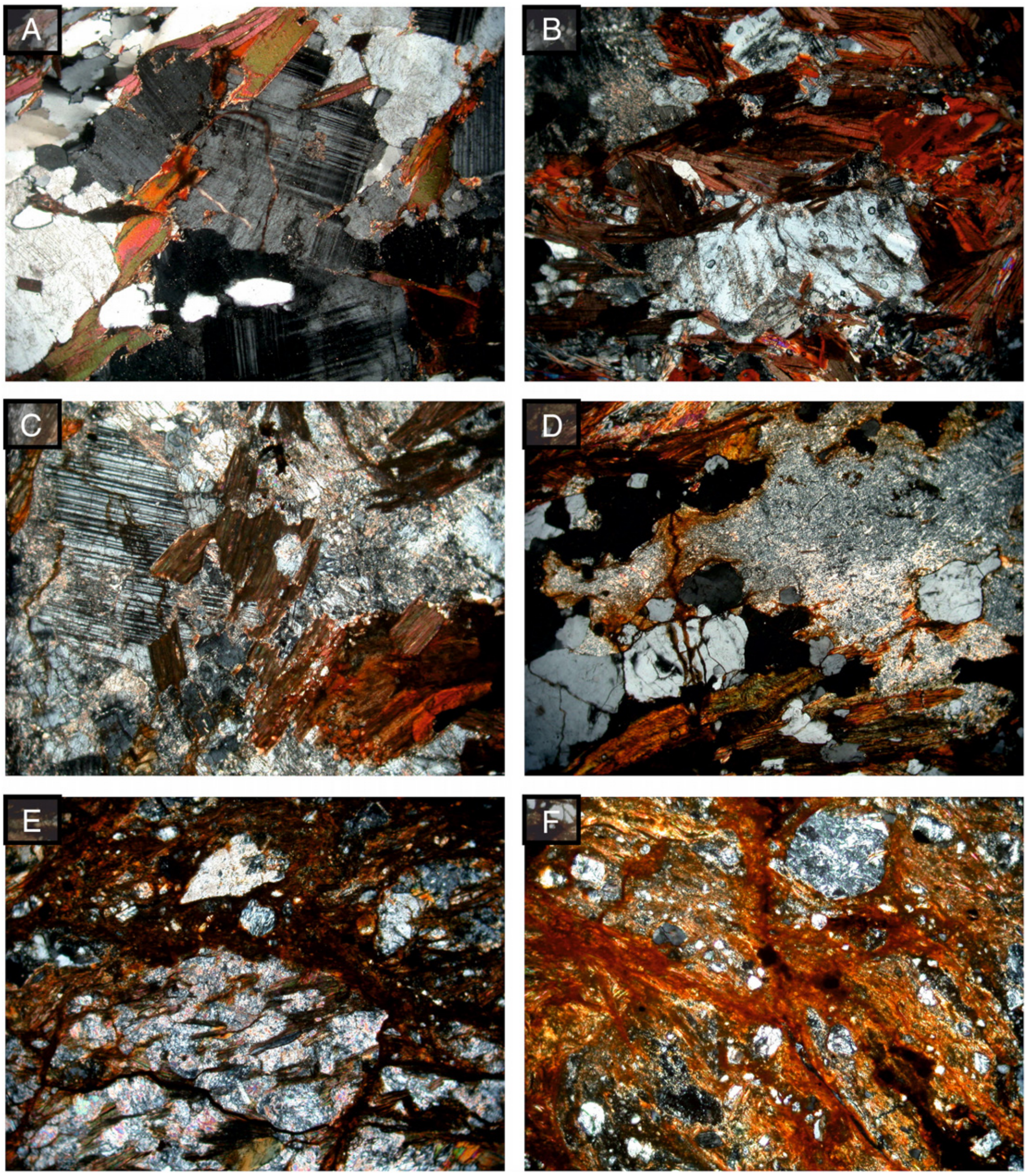

Fig. 6. Photomicrographs of weathering stages for the studied gneiss (crossed polarized light). A) fresh rock (class I) (10×); B) slightly weathered sample (class II) (10×); C) moderately weathered sample (class III) (10×); D) highly weathered sample (class IV) (10×); E) completely weathered sample (class V) (10×); F) completely weathered sample characterized by clasts in an oxidized and argillaceous matrix (classes V–VI) (10×).

have been recognized for the M-G samples (Table 1), whereas the BGS-G samples are mainly characterized by higher I_p indices (Table 1) typical of fresh (e.g., Fig. 6A) or slightly weathered (e.g., Fig. 6B) and moderately weathered rocks (e.g., Fig. 6C). Samples from class III to class IV show petrological changes characterized by a nearly complete alteration of plagioclase and biotite and a slight decomposition of K-feldspar. Class V comprises samples intensely microfractured by transgranular microcracks (e.g., Fig. 7G), contributing to the increase of rock porosity, with clay-coated feldspar grains. Thus, the highest weathering stages (classes V–VI) are characterized by strong petrological changes, and extreme microfracturing, which are typical of soil material behavior (Irfan and Dearman, 1978).

6. Discussion

In the Sila massif the geomorphological, compositional, textural and mechanical evidence all support the idea that both physical disintegration and chemical alteration affect metamorphic rock masses (e.g., Le Pera and Sorriso-Valvo, 2000a). It has been demonstrated that, in a humid climate, chemical weathering acts vigorously on sediment composition derived from crystalline rocks, destroying labile minerals, such as feldspar and Fe–Mg phases, and lithic fragments (Grantham and Velbel, 1988; Nesbitt and Young, 1989). Quartz is much more resistant to chemical weathering and it increases in relative abundance in the more humid climates because of the release of quartz grains from the weathering of the rock fragments (Young et al., 1975).

Nesbitt and Young (1996), Fedo et al. (1995) and Nesbitt et al. (1996) show that feldspar depletion becomes progressively more pronounced as chemical weathering proceeds, and the resulting samples become progressively less representative of the source rock mineralogy, and shifted toward a quartzose composition with enrichment in clay minerals. Based on compositional and textural features of the studied samples, the initial stage of weathering produces mainly precipitates of Fe-oxides along biotite cleavage planes (Fig. 8A); thus, ferrous (Fe^{2+}) iron of the iron-bearing silicates is combined with oxygen

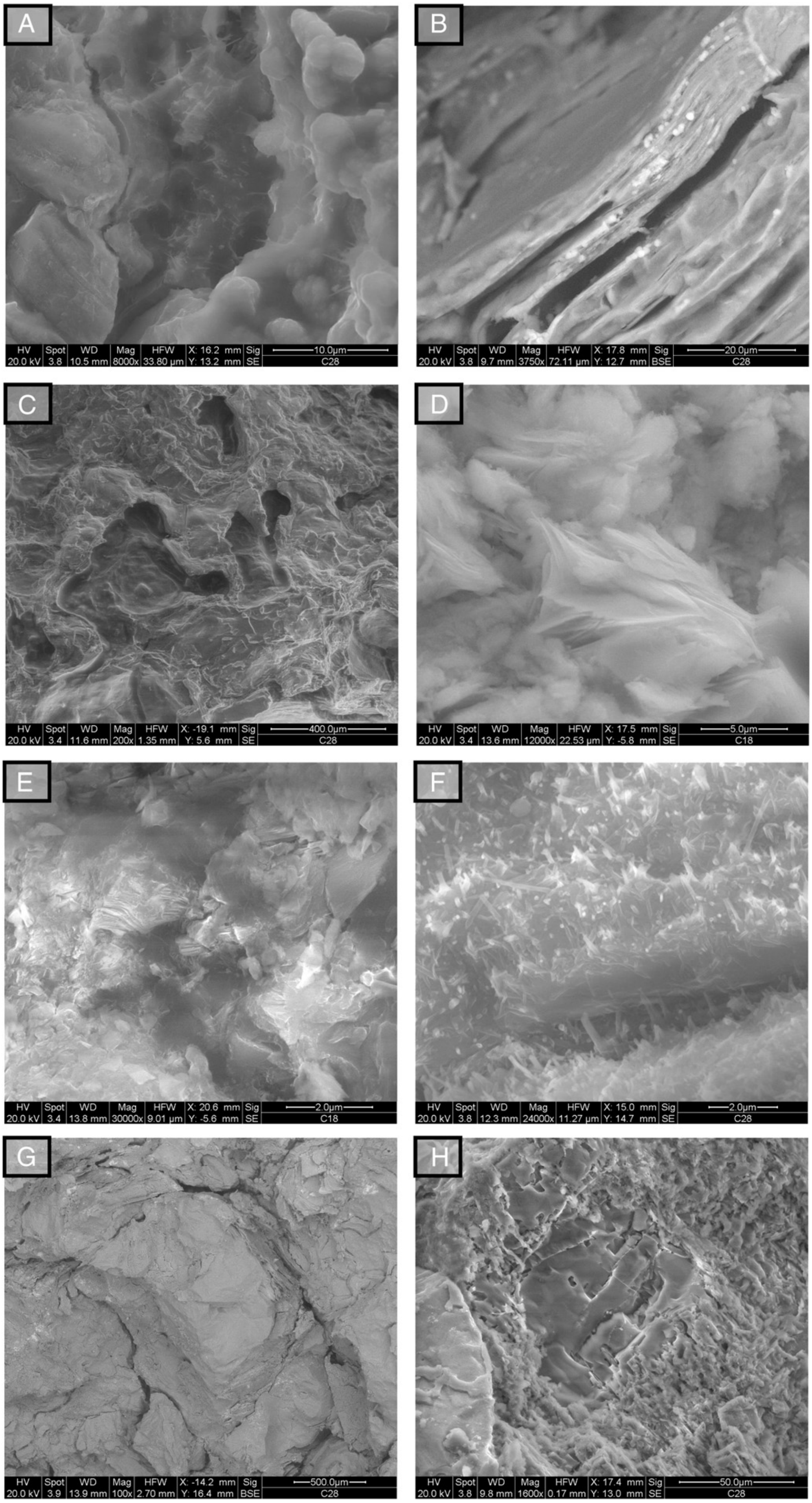
A
HV 20.0 kV | Spot 3.8 | WD 10.5 mm | Mag 8000x | HFW 33.80 µm | X: 16.2 mm Y: 13.2 mm | Sig SE | 10.0µm | C28
B
HV 20.0 kV | Spot 3.8 | WD 9.7 mm | Mag 3750x | HFW 72.11 µm | X: 17.8 mm Y: 12.7 mm | Sig BSE | 20.0µm | C28
C
HV 20.0 kV | Spot 3.4 | WD 11.6 mm | Mag 200x | HFW 1.35 mm | X: -19.1 mm Y: 5.6 mm | Sig SE | 400.0µm | C28
D
HV 20.0 kV | Spot 3.4 | WD 13.6 mm | Mag 12000x | HFW 22.53 µm | X: 17.5 mm Y: -5.8 mm | Sig SE | 5.0µm | C18
E
HV 20.0 kV | Spot 3.4 | WD 13.8 mm | Mag 30000x | HFW 9.01 µm | X: 20.6 mm Y: -5.6 mm | Sig SE | 2.0µm | C18
F
HV 20.0 kV | Spot 3.8 | WD 12.3 mm | Mag 24000x | HFW 11.27 µm | X: 15.0 mm Y: 14.7 mm | Sig SE | 2.0µm | C28
G
HV 20.0 kV | Spot 3.9 | WD 13.9 mm | Mag 100x | HFW 2.70 mm | X: -14.2 mm Y: 16.4 mm | Sig BSE | 500.0µm | C28
H
HV 20.0 kV | Spot 3.8 | WD 9.8 mm | Mag 1600x | HFW 0.17 mm | X: 17.4 mm Y: 13.0 mm | Sig SE | 50.0µm | C28

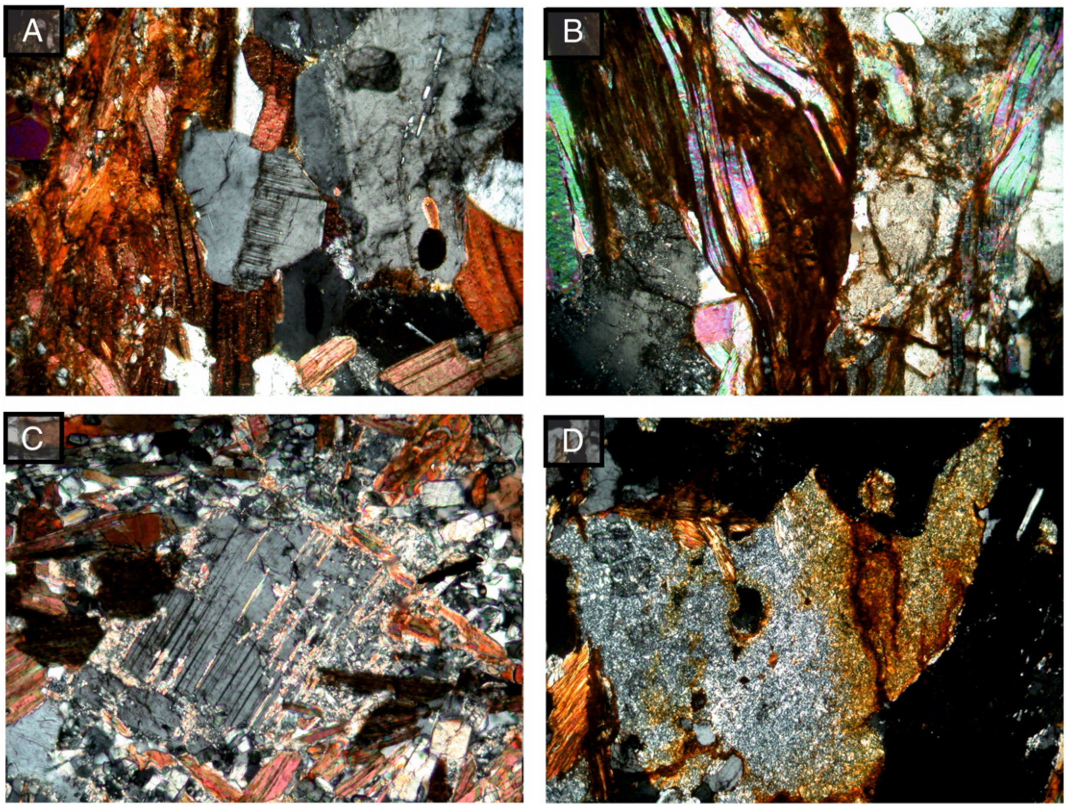

Fig. 8. Stages of mineral (biotite and plagioclase) alteration (crossed polarized light). A) Early stage of biotite alteration characterized by incipient clay mineral formation and Fe-oxides along cleavage planes (20×); B) more advance stage of biotite alteration replaced by Fe-oxides and abundant clay minerals along rims and lamellae (20×); C) early stage of plagioclase alteration showing fine-grained sericite along twin planes (20×); D) more advance stage of plagioclase alteration with pervasive sericite and neoformed clay minerals (20×).

to form ferric (Fe^{3+}) iron oxides (e.g., hematite) (Fig. 8B). Furthermore, newly formed clay minerals (chlorite), replacing biotite along rims and lamellae (Fig. 8B), has also been observed in a later stage of biotite weathering (e.g., Stoch and Sikora, 1976).

Fine-grained sericite often occurs within plagioclase, preferentially along twin planes (Fig. 8C), or more pervasively, as bright yellowish birefringent laths a few microns in size. A pre-weathering origin for sericite has been considered (Dixon and Young, 1981; James et al., 1981; Velbel, 1983), even if a formation during deep weathering conditions cannot be ruled out (Irfan and Dearman, 1978; Ollier, 1983, 1984, 1988). As weathering advances, clay minerals replace fine-grained sericite, preferentially along mineral rims (Fig. 8D).

Furthermore, these newly formed phases along cleavage planes expand the mineral, thereby producing a wedge effect which fractures adjacent grain (e.g., Baynes and Dearman, 1978a; Eggler et al., 1969). The advanced stage of weathering is marked by chemical breakdown and weathering of feldspar. Feldspars have an opaque, brownish appearance, due to a microcrystalline secondary product, that is probably a clay mineral replacement during weathering (e.g., Le Pera et al., 2001; Tazaki and Fyfe, 1987; Velbel, 1983). All these processes influence the rock microfabric, increasing crystal microfracturing and rock disaggregation with a decrease of the physical–mechanical properties (e.g., Cascini et al., 1994; Heins, 1995; Le Pera et al., 2001 and references therein).

The X-ray diffraction pattern of the completely weathered sample shows the occurrence of neoformed clay minerals, typically large amounts of interstratified clay minerals (both 2:1 and 2:1:1 clay minerals), chlorite, micas and 1:1 clay minerals (Fig. 9). The difference between the fresh rock and the completely weathered rock XRD pattern is mainly related to the abundance of feldspars, which decrease from fresh to completely weathered samples, and clay minerals, that are neoformed in the completely weathered sample (Fig. 9). These observations confirm the minero-petrographic considerations mentioned above.

As observed in this study, the lower values of the decomposition index (X_d), that mainly characterize the BGS-G samples (Table 1), reflect a granular framework microfabric of the gneiss, consisting of dominant sand and silt fraction, and a lower percentage of clay. The progressive weathering stage is outlined by the occurrence of a clay-matrix microfabric, as showed by the M-G samples having commonly higher X_d values and lower I_p values (Table 1). However, in the studied samples (BGS-G and M-G) occur both granular framework and clay-matrix microfabric; the contemporaneous presence of both granular- and clay-matrix microfabric reflects a complex weathering profile development, combined with a varying amount of eluviation (e.g., Baynes and Dearman, 1978a; Teeuw et al., 1994).

The gneiss framework microfabric is mainly related to the severe fracturing and faulting that occur in the studied weathering profiles (Figs. 3–4). These processes furthermore produce the loss of resistance in the rock that is one of the most factors predisposing the mass movement phenomena in the Sila gneiss (e.g. Borrelli et al., 2007; Cascini et al., 1994). The relationship between mass movement and weathering state regards also the presence of neoformed clay minerals; among these the presence of abundant halloysite, that is a

Fig. 7. SEM photographs of weathering features. A) argillification (neoformed clay minerals) of plagioclase; B) Fe-oxide replacement in biotite; C) mineral dissolution process; D) neoformed platy illite minerals; E) booklets of kaolinite; F) tabular morphology of halloysite; G) incipient disintegration indicated by transgranular and intragranular microcracks; H) feldspar grain chemical alteration.

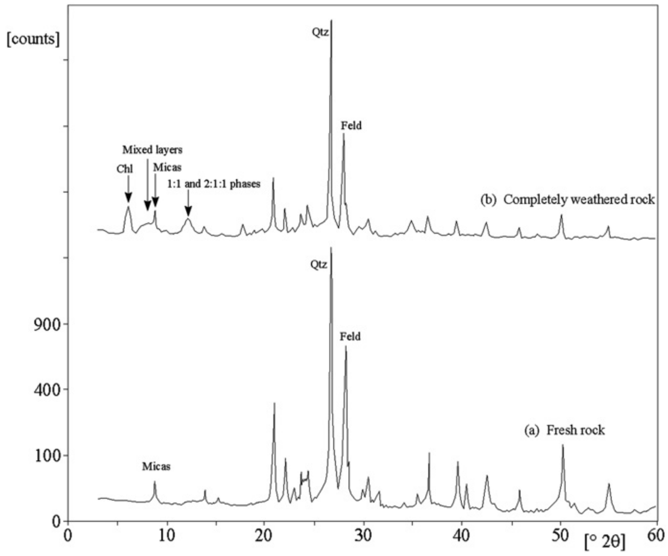

Fig. 9. X-ray diffraction patterns for fresh (sample C94) and completely weathered (sample C98) bulk samples. Qtz: quartz, Feld: feldspars, Chl: chlorite.

swelling clay mineral, in the completely weathered rocks and residual soils, that may decrease slope instability (e.g., Cascini et al., 1994 and references therein).

Generally, the type of clay mineral neoformed from the source rock may change as a function of climate, relief, rainfall, drainage, original rock type, vegetation and weathering time. Bates (1962) illustrates that clay minerals composed of the more soluble elements (e.g., smectite) are formed in environments where these ions can accumulate and, thus, in a poorly drained areas of low relief (e.g., Hong et al., 2010); these environments are characterized by lower rainfall in a warm/dry climate. On the other hand, clays composed of the least soluble elements (e.g., gibbsite) form under severe leaching conditions (e.g., climate characterized by very high rainfall conditions). Halloysite predominates in zones with intermediate rainfall; kaolinite forms in intermediate zones (characterized by wet–humid conditions) where silicon, as well as aluminum, can be retained (e.g., Eberl, 1984; Thompson et al., 1982). Halloysite and kaolinite may often coexist in the upper parts of the gneissic weathering profiles developed under a temperate climate (Papoulis et al., 2004), as the Mediterranean environment. Chlorite forms under a variety of physical and chemical weathering conditions (e.g., Slaughter and Milne, 1960; Weaver, 1989). Illite mainly exists in areas of very low rates of chemical weathering with cooler climate, and areas of steep relief where mechanical erosion interferes with soil formation (Chamley, 1989; Weaver, 1989).

The presence of these neoformed clay minerals (kaolinite, halloysite, chlorite and illite) in the studied samples, as showed by thin section, SEM and XRD analyses, reflects an alternation between chemical weathering and mechanical erosion (as also showed by microcracks and rock disaggregation) and furthermore suggests an alternation of wet–humid conditions with cooler season (e.g., Gerrard, 1994). Thus, the development of the weathering of land surface could be a result of intense tectonic uplift and climatic oscillations since, at least, the Pleistocene time (Le Pera and Sorriso-Valvo, 2000b; Le Pera et al., 2001; Nossin, 1973).

The tectonic uplift mainly related to important regional fault systems, played an important role in the Neogene–Quaternary geodynamic evolution of the central Mediterranean area (e.g., Tansi et al., 2007). The presence of these fault systems may influence the morphology and the features of the weathering profiles. In particular, many fractured zone associated to fault planes and completely degraded rocks associated to thrust planes have been observed along the borehole logs studied (Figs. 4 and 5), where physical and chemical weathering produce argillified levels. The association among fractured zones and completely degraded rocks with argillified portions represents a predisposing factor to the development of mass movements such as, in particular, DSGSD (Deep Seated Gravitational Slope Deformation) and deep landslides.

7. Conclusions

This study concerns the importance of chemical and physical weathering in the morphogenic processes and landscape evolution along gneissic weathering profiles of the Sila Massif (Calabria, southern Italy). There is a general relationship between the sediment yield of a major denudation region, and the history of the weathering, climate and topography of a mountainous region such as Calabria. The evolution of the studied weathering profiles is related to a source area with high precipitation rate, abruptly changing topography, weathered metamorphic rocks, and where residence time of soils is dependent upon topography.

The surveys and analyses conducted in this study according to a multidisciplinary approach revealed a complex history of the weathering profiles. Significant results were achieved by applying mineralogical and petrographical assessment criteria. The studied gneissic weathering profiles are characterized by six stages of weathering, starting from fresh rock samples to completely weathered samples where chemical decompositions, clasts in an oxidized and argillaceous matrix and neoformed clay minerals prevails. All these weathering stage transitions are well documented by X_d values and the micropetrographic index *I*p and by SEM and thin-section images and XRD patterns. These changes are related to the type of microfabrics, mainly granular (or clay-poor) for the BGS-G samples and clay-rich for the M-G samples, that substitute the original rock fabric. These data, based on X_d values and the micropetrographic index *I*p and mineralogical analyses, confirm the results obtained by the detailed field survey of the weathering grade on cut slopes.

The mineralogical characteristics of the weathered bedrock show that hilltop (i.e. minimum slope angle detritus; Le Pera and Sorriso-Valvo, 2000b) is more evolved. Correlation between weathering profile mineralogy and texture and current climate suggests that the alteration process is still active under present-day conditions.

Furthermore, the results achieved in this study on the weathering profile evolution provide a useful tool to gain insight into the geomorphological evolution and phenomenon–cause–effect relation regarding the investigation on landsliding events.

Acknowledgments

This work is part of the research project entitled 'Typing of natural events with a high social and economic impact' of the CNR-Istituto di Ricerca per la Protezione Idrogeologica nell'Italia Meridionale ed Insulare, Italy. The authors are very grateful to two anonymous reviewers for their reviews and suggestions on the manuscript.

References

Amodio-Morelli, L., Bonardi, G., Colonna, V., Dietrich, D., Giunta, G., Ippolito, F., Liguori, V., Lorenzoni, S., Paglionico, A., Perrone, V., Piccarreta, G., Russo, M., Scandone, P., Zanettin-Lorenzoni, E., Zuppetta, A., 1976. L'Arco Calabro–Peloritano nell'orogene appennino-magrebide. Memorie della Società Geoligica Italiana 17, 1–60.

Baynes, F.J., Dearman, W.R., 1978a. The microfabric of a chemically weathered granite. Bulletin of the International Association of Engineering Geology 18, 91–100.

Baynes, F.J., Dearman, W.R., 1978b. The relationship between the microfabric and the engineering properties of weathered granite. Bulletin of the International Association of Engineering Geology 18, 191–197.

Bates, T., 1962. Halloysite and gibbsite formation in Hawaii. Clays and Clay Minerals 9, 315–328.

Borrelli, L., 2008. Categorie di frane ed elementi caratteristici nei profili di alterazione. PhD Thesis. University of Calabria. 395 pp.

Borrelli, L., Greco, R., Gullà, G., 2007. Weathering grade of rock masses as a predisposing factor to slope instabilities: reconnaissance and control procedure. Geomorphology 87, 158–175.

Brand, E.W., Phillipson, H.B., 1985. Sampling and testing of residual soils: a review of international practice: 1–194. Technical Committee on Sampling and Testing of Residual Soils, International Society for Soil Mechanics and Foundation Engineering. Scorpion Press.

Caggianelli, A., Del Moro, A., Piccarreta, G., 1994. Petrology of basic and intermediate orogenic granotoids from the Sila Massif (Calabria, southern Italy). Geological Journal 29, 11–28.

Calcaterra, D., Bruno, D.E., Parise, M., Silvestri, F., Critelli, S., Capparelli, G., 2004. Effects of weathering on slope instability in gneissic rocks at Luzzi (Calabria, Italy). Proceedings of the 9th International Symposium on Landslides, Rio de Janeiro, pp. 1233–1239.

Calcaterra, D., Parise, M., Dattola, L., 1998. Weathering processes in crystalline rocks of the Sila Massif, Calabria, southern Italy, as predisposing factor for the development of debris flows. Proc. 2nd Int. Symp. In: Evangelista, A., Picarelli, L. (Eds.), The Geotechnics of Hard Soils, pp. 73–84. Naples, Italy.

Calcaterra, D., Parise, M., Dattola, L., 1996. Caratteristiche dell'alterazione e franosita di rocce granitoidi nel bacino del Torrente Alaco (massiccio delle Serre, Calabria). Bollettino. Societa Geologica Italiana 115, 3–28.

Caracciolo, L., Le Pera, E., Muto, F., Perri, F., 2011. Sandstone petrology and muddstone geochemistry of the Peruc-Korycany Formation (Bohemien Cretaceous Basin, Czech Republic). International Geology Review 53, 1003–1031.

Cascini, L., Critelli, S., Di Nocera, S., Gullà, G., Matano, F., 1994. Weathering and landsliding in Sila Massif gneiss (Northern Calabria, Italy). Proceedings of the 7th International IAEG Congress, Lisboa, Portugal, pp. 1613–1622.

Cascini, L., Gullà, G., 1993. Caratterizzazione fisico-meccanica dei terreni prodotti dall'alterazione di rocce gneissiche. Rivista Italiana di Geotecnica 2, 125–147.

Cascini, L., Critelli, S., Di Nocera, S., Gulla, G., Matano, F., 1992. Grado di alterazione e franosita negli gneiss del massiccio silano: l'area di San Pietro in Guarano (CS). Geología Applicata e Idrogeología 27, 49–76.

Cavalcante, F., Fiore, S., Lettino, A., Piccarreta, G., Tateo, F., 2007. Illite–smectite mixed layer in Sicilide shales and piggy-back deposits of the Gorgoglione Formation (Southern Apennines): geological inferences. Bollettino. Societa Geologica Italiana 103, 241–254.

Chamley, H., 1989. Clay Sedimentology. Springer, Heidelberg. 623 pp.

Critelli, S., Mongelli, G., Perri, F., Martìn-Algarra, A., Martìn-Martìn, M., Perrone, V., Dominici, R., Sonnino, M., Zaghloul, M.N., 2008. Compositional and geochemical signatures for the sedimentary evolution of the Middle Triassic–Lower Jurassic continental redbeds from Western-Central Mediterranean Alpine Chains. Journal of Geology 116, 375–386.

Critelli, S., Di Nocera, S., Le Pera, E., 1991. Approccio metodologico per la valutazione petrografica del grado di alterazione degli gneiss del Massiccio Silano (Calabria settentrionale). Geología Applicata e Idrogeología 26, 41–70.

Deere, D.U., Patton, F.D., 1971. Slope stability in residual soils. Proceedings of the 4th Pan American Conference on Soil Mechanics and Foundation Engineering, San Juan, Puerto Rico, pp. 87–170.

Dixon, J.C., Young, R.W., 1981. Character and origin of deep arenaceous weathering mantles on the Bega Batholith, southeastern Australia. Catena 8, 97–109.

Eberl, D.D., 1984. Clay mineral formation and transformation in rocks and soils. Philosophical Transactions of the Royal Society of London 311, 241–257.

Eggler, D.H., Larson, E.E., Bradley, W.C., 1969. Granites, grusses, and the Sherman erosion surface, southern Laramie Range, Colorado–Wyoming. American Journal of Science 267, 510–522.

Fedo, C.M., Nesbitt, H.W., Young, G.M., 1995. Unraveling the effect of potassium metasomatism in sedimentary rocks and paleosols, with implications for paleoweathering conditions and provenance. Geology 23, 921–924.

Gerrard, J., 1994. Weathering of granitic rocks: environment and clay mineral formation. In: Robinson, D.A., Williams, R.B.G. (Eds.), Rock Weathering and Landform Evolution. Wiley, New York, pp. 3–20.

Grantham, J.H., Velbel, M.A., 1988. The influence of climate and topography on rock-fragment abundance in modern fluvial sands of the southern Blue Ridge Mountains, North Carolina. Journal of Sedimentary Petrology 58, 219–227.

Gullà, G., Critelli, S., Aceto, L., Perri, F., 2008. Geotechnical and mineralogical characterisation of fine-grained soils affected by soil slips. In: Chen, et al. (Ed.), Landslides and Engineered Slopes. Taylor & Francis Group, London, pp. 373–379.

Gullà, G., Borrelli, L., Greco, R., 2004. Weathering of rock-mass as possible characterizing factor of predisposition to slope instabilities. Proceedings of the IX International Symposium on Landslides, Rio de Janeiro, pp. 103–108.

Gullà, G., Matano, F., 1997. Surveys of weathering profile on gneiss cutslopes in Northern Calabria, Italy. Proceedings of the International Symposium on Engineering Geology and the Environment, IAEG, Athens, Greek, pp. 133–138.

Gullà, G., Matano, F., 1994. Proposta di una procedura per il rilievo del grado di alterazione di gneiss su fronti rocciosi. Geologica Romana 30, 227–238.

Guzzetta, G., 1974. Ancient tropical weathering in Calabria. Nature 251, 302–303.

Hencher, S.R., Massey, J.B., Brand, E.W., 1984. Application of back analysis to some Hong Kong landslides. Proceedings of the 4th International Symposium on Landslides, Toronto, pp. 631–638.

Heins, W.A., 1995. The use of mineral interfaces in sand-sized rock fragments to infer ancient climate. Geological Society of America Bulletin 107, 113–125.

Hill, S.E., Rosenbaum, M.S., 1998. Assessing the significant factors in a rock weathering system. Quarterly Journal of Engineering Geology 31, 85–94.

Hong, H., Zhang, K., Li, Z., 2010. Climatic and tectonic uplift evolution since ~7 Ma in Gyirong basin, south-western Tibet plateau: clay mineral evidence. International Journal of Earth Sciences (Geol. Rundsch) 99, 1305–1315.

Irfan, T.Y., Dearman, W.R., 1978. The engineering petrography of a weathered granite in Cornwall, England. Quarterly Journal of Engineering Geology 11, 223–244.

James, W.C., Mack, G.H., Suttner, L.J., 1981. Relative alteration of microcline and sodic plagioclase in semi-arid and humid climates. Journal of Sedimentary Petrology 51, 151–164.

Köppen, W., 1936. Das geographische System der Klimate. In: Köppen, W., Geiger, R. (Eds.), Handbuch der Klimatologie, Band 5, Teil C. Gebrüder Bornträger, Berlin, pp. 1–46.

Lacerda, W.A., Santos, J.R., 2000. Water table fluctuation — a cause of slide initiation in residual and colluvial soils in tropical regions. Proceedings of the 8th International Symposium on Landslides, Cardiff, pp. 877–880.

Lee, S.G., De Freitas, D.H., 1989. A revision of the description and classification of weathered granite and its application to granite in Korea. Quarterly Journal of Engineering Geology 22, 31–48.

Le Pera, E., Critelli, S., Sorriso-Valvo, M., 2001. Weathering of gneiss in Calabria, Southern Italy. Catena 42, 1–15.

Le Pera, E., Sorriso-Valvo, M., 2000a. Weathering and morphogenesis in a mediterranean climate, Calabria, Italy. Geomorphology 34, 251–270.

Le Pera, E., Sorriso-Valvo, M., 2000b. Weathering, erosion and sediment composition in a high-gradient river, Calabria, Italy. Earth Surface Processes and Landforms 25, 277–292.

Lumb, P., 1962. The properties of decomposed granite. Geotecnique 12, 226–243.

Messina, A., Russo, S., Borghi, A., Colonna, V., Compagnoni, R., Caggianelli, A., Fornelli, A., Piccarreta, G., 1994. Il Massiccio della Sila Settore settentrionale dell'Arco Calabro-Peloritano. Bollettino. Societa Geologica Italiana 113, 539–586.

Messina, A., Barbieri, M., Compagnoni, R., De Vivo, B., Perrone, V., Russo, S., Scott, B.A., 1991. Geological and petrochemical study of the Sila Massif plutonic rocks (Northern Calabria, Italy). Bollettino. Societa Geologica Italiana 110, 165–206.

Mongelli, G., Critelli, S., Perri, F., Sonnino, M., Perrone, V., 2006. Sedimentary recycling, provenance and paleoweathering from chemistry and mineralogy of Mesozoic continental redbed mudrocks, Peloritani Mountains, Southern Italy. Geochemical Journal 40, 197–209.

Mongelli, G., Cullers, R.L., Dinelli, E., Rottura, A., 1998. Elemental mobility during the weathering of exposed lower crust: the kinzigitic paragneisses from the Serre, Calabria, Southern Italy. Terra Nova 10, 190–195.

Moore, D.M., Reynolds, R.C., 1997. X-Ray Diffraction and the Identification and Analysis of Clay Minerals, Second Edition. Oxford University Press, New York. 378 pp.

Nesbitt, H.W., Young, G.M., McLennan, S.M., Keays, R.R., 1996. Effects of chemical weathering and sorting on the petrogenesis of siliciclastic sediments, with implications for provenance studies. Journal of Geology 104, 525–542.

Nesbitt, H.W., Young, G.M., 1996. Petrogenesis of sediments in the absence of chemical weathering: effects of abrasion and sorting on bulk composition and mineralogy. Sedimentology 43, 341–358.

Nesbitt, H.W., Young, G.M., 1989. Formation and diagenesis of weathering profiles. Journal of Geology 97, 129–147.

Nesbitt, H.W., Young, G.M., 1982. Early Proterozoic climates and plate motions inferred from major element chemistry of lutites. Nature 299, 715–717.

Nishida, K., Aoyama, C., 1985. Weathered residual soil properties and failure mechanism of slope. Proceedings of the 4th International Conference and Field Workshop on Landslides, Tokyo, pp. 289–294.

Nossin, J.J., 1973. Use of air photos in studies of slope stability in the Crati basin Calabria, Italy. Geología Applicata e Idrogeología 8, 261–287.

Ollier, C., 1988. The regolith in Australia. Earth-Science Reviews 25, 355–361.

Ollier, C., 1984. Weathering, 2nd ed. Longman, New York.

Ollier, C., 1983. Weathering or hydrothermal alteration? Catena 10, 57–59.

Palmentola, G., Acquafredda, P., Fiore, S., 1990. A new correlation of the glacial moraines in the southern Appennines, Italy. Geomorphology 3, 1–8.

Papoulis, D., Tsolis-Katagas, P., Katagas, C., 2004. Progressive stages in the formation of kaolin minerals of different morphologies in the weathering of plagioclase. Clays and Clay Minerals 52, 275–286.

Perri, F., Cirrincione, R., Critelli, S., Mazzoleni, P., Pappalardo, A., 2008. Clay mineral assemblages and sandstone compositions of the Mesozoic Longobucco Group (north-eastern Calabria): implication for burial history and diagenetic evolution. International Geology Review 50, 1116–1131.

Perri, F., Critelli, S., Mongelli, G., Cullers, R.L., 2011. Sedimentary evolution of the Mesozoic continental redbeds using geochemical and mineralogical tools: the case of Upper Triassic to Lowermost Jurassic Monte di Gioiosa mudrocks (Sicily, southern Italy). International Journal of Earth Sciences 100, 1569–1587.

Perri, F., Mongelli, G., Sonnino, M., Critelli, S., Perrone, V., 2005. Chemistry and mineralogy of mesozoic continental redbed mudrocks from the Calabrian Arc, Southern Italy: implication for provenance, paleoweathering and burial history. Atti Ticinensi di Scienze della Terra 10, 103–106.

Perri, F., 2006. Analisi geochimica, mineralogia e petrografia di successioni sedimentarie triassico-giurassiche del rifting tetideo, dell'Arco Calabro-Peloritano: implicazioni sulla loro storia evolutiva. [unpubl. Ph.D. thesis]: Università della Basilicata, 210 pp.

Perri, F., 2008. Clay mineral assemblage of the Middle Triassic–Lower Jurassic mudrocks from Western-Central Mediterranean Alpine Chains. Periodico di Mineralogia 77, 23–40.

Price, D.G., 1995. Weathering and weathering processes. Quarterly Journal of Engineering Geology 28, 243–252.

Slaughter, M., Milne, I.H., 1960. The formation of chlorite-like structures from montmorillonite. Clays and Clay Minerals 5, 114–124.

Sorriso-Valvo, M., Gabriele, S., Gullà, G., Antronico, L., Tansi, C., Aceto, L., Dodaro, F., Greco, R., Niceforo, D., Fantucci, R., 2005. Studio geologico–geomorfologico–geotecnico e monitoraggio della frana di Serra di Buda (Acri). CNR-IRPI, Regione Calabria LL.PP. e Acque, Autorità di Bacino Regione Calabria. Rubbettino Editore.

Stoch, L., Sikora, W., 1976. Transformation of micas in the process of kaolinization of granites and gneiss. Clays and Clay Minerals 24, 156–162.

Stoops, J., 2003. Guidelines for Analysis and Description of Soil and Regolith Thin Sections. Soil Science Society of America, Inc., Madison, Wisconsin USA.

Tansi, C., Muto, F., Critelli, S., Iovine, G., 2007. Neogene–Quaternary strike-slip tectonics in the central Calabrian Arc (southern Italy). Journal of Geodynamics 43, 393–414.

Tazaki, K., Fyfe, W.S., 1987. Primitive clay precursors formed on feldspar. Canadian Journal of Earth Sciences 24, 506–527.

Teeuw, R.M., Thomas, M.F., Thorp, M.B., 1994. Regolith and landscape development in the Koidu basin of Sierra Leone. In: Robinson, D.A., Williams, R.B.G. (Eds.), Rock Weathering and Landform Evolution. Wiley, New York, pp. 303–320.

Terranova, O., Antronico, L., Gullà, G., 2007. Landslide triggering scenarios in homogeneous geological contexts: the area surrounding Acri (Calabria, Italy). Geomorphology 87, 250–267.

Thomas, M.F., 1994. Geomorphology in the Tropics: A Study of Weathering and Denudation in Low Latitudes. John Wiley and Sons, New York. 460 pp.

Thompson, G.R., Fields, R.W., Alt, D., 1982. Land-based evidence for Tertiary climatic variations: Northern Rockies. Geology 10, 413–417.

Thomson, S.N., 1994. Fission-track analysis of the crystalline basement rocks of the Calabrian Arc, southern Italy: evidence of Oligo-Miocene late-orogenic extension and erosion. Tectonophysics 238, 331–352.

Tsidzi, K.E.N., 1986. A quantitative petrofabric characterization of metamorphic rocks. Bulletin of the International Association of Engineering Geology 33, 3–12.

Velbel, M.A., 1983. A dissolution–reprecipitation mechanism for the pseudomorphous replacement of plagioclase feldspar by clay minerals during weathering. Petrologie des Alterations et des Sols, vol. I. In: Nahon, D., Noack, Y. (Eds.), Sc. Geol. Mem. (Strasbourg), 71, pp. 139–147.

Weaver, C.E., 1989. Clays, muds, and shales. Developments in Sedimentology, vol. 44. Elsevier, Amsterdam. 819 pp.

Young, S.W., Basu, A., Mack, G.H., Darnell, N., Suttner, L.J., 1975. Use of size ± composition trends in Holocene soil and fluvial sand for paleoclimate interpretation. Proceedings of the 9th International Sedimentological Congress, Theme 1, Nice, France, pp. 201–209.

Zaghloul, M.N., Critelli, S., Perri, F., Mongelli, G., Perrone, V., Sonnino, M., Tucker, M., Aiello, M., Ventimiglia, C., 2010. Depositional systems, composition and geochemistry of Triassic rifted-continental margin redbeds of Internal Rif Chain, Morocco. Sedimentology 57, 312–350.